Cell. Mol. Biol. (ISSN: 1165-158X)

Journal Homepage: www.cellmolbiol.org

Cellular and Molecular Biology

Original Article

Chelidonium majus L. alkaloid extract encapsulated in human serum albumin nanoparticles induces mitochondria-mediated apoptosis in HeLa cell line

Mahdieh Imani[1], Masoud Parsania[2, 3*], Fatemeh Rouhollah[1*], Mohammad Hassan Pouriayevali[4]

[1] Department of Cellular and Molecular Biology, TeMS.C., Islamic Azad University, Tehran, Iran
[2] Department of Microbiology, TeMS.C., Islamic Azad University, Tehran, Iran
[3] Medical Genomics Research Center, TeMS.C., Islamic Azad University, Tehran, Iran
[4] Department of Arboviruses and Viral Hemorrhagic Fevers (National Reference Laboratory), Pasteur Institute of Iran, Tehran, Iran

Article Info

Article history:

Received: February 27, 2026
Accepted: April 25, 2026
Published: May 31, 2026

Use your device to scan and read the article online

Abstract

Interest in herbal medicines as complementary therapies has increased because of concerns regarding the adverse effects of conventional chemotherapeutic agents. Chelidonium majus L. (C. majus) exhibits antiproliferative activity against several cancer cell lines; however, its therapeutic efficacy may be limited by poor bioavailability. This study evaluated the apoptotic activity of C. majus alkaloid extract encapsulated in human serum albumin nanoparticles (C. majus/HSA-NPs) in HeLa cervical cancer cells. Cytotoxicity of C. majus alkaloid extract (C. majus/AE), C. majus/HSA-NPs, and HSA-NPs was determined using the MTT assay in HeLa and human fibroblast cells, apoptosis was quantified by Annexin V/PI flow cytometry, and the mRNA expression of Bax, Bcl-2, caspase-9 and caspase-3 was analyzed by real-time RT-PCR. After 48 h, the IC_{50} values in HeLa cells were 70.79 µg/mL for C. majus/AE, 52.37 µg/mL for C. majus/HSA-NPs, and >2000 µg/mL for HSA-NPs, whereas fibroblast cells exhibited substantially higher IC_{50} values (835 µg/mL for C. majus/AE and >1600 µg/mL for both C. majus/HSA-NPs and HSA-NPs), indicating selective cytotoxicity toward cancer cells. C. majus/HSA-NPs induced significantly greater apoptosis than the free alkaloid extract and markedly enhanced the expression of the pro-apoptotic genes Bax, caspase-9, and caspase-3, while suppressing **Bcl-2**, resulting in a significantly higher Bax/Bcl-2 ratio, consistent with activation of the mitochondrial apoptotic pathway. Overall, nanoencapsulation with human serum albumin enhanced the anticancer efficacy of C. majus alkaloids while maintaining low toxicity toward normal fibroblasts, suggesting that C. majus/HSA-NPs represent a promising candidate for targeted cervical cancer therapy, although further in vivo and mechanistic studies are required to confirm their therapeutic potential.

Keywords: *C. majus* alkaloids; Human serum albumin; nanoparticles; Apoptosis; HeLa cells.

1. Introduction

Cervical cancer (CC) is the second most common cancer affecting females in less developed countries, and the most important cause of cervical cancer is HPV [1]. The research conducted on cervical cancer has predominantly utilized the HeLa cell line, a pivotal model in these cancer studies. The HeLa cell line is recognized as the oldest and most widely used human cell line in scientific research [2]. Various diseases, such as autoimmunity and cancer, can be caused by defects in the function or inhibition of the apoptosis process and improper upregulation or downregulation of apoptosis. Apoptosis helps to destroy virus-infected cells and also to destroy damaged cells [3].

In cancer, insufficient apoptosis allows malignant cells to survive and proliferate. Understanding the effect of apoptosis on these diseases is essential for developing effective treatments. The apoptosis pathway can be activated by two groups of intracellular and extracellular signals known as the death receptor pathway and the mitochondrial pathway[4]. The intrinsic apoptotic pathway uses mitochondrial proteins. Various stimuli, such as cells with damaged DNA or oncogenes, can trigger the intrinsic apoptotic pathway. Bcl-2 family proteins are capable of regulating cellular processes by controlling mitochondrial outer membrane permeability. Upon stimulation, Bax and Bak proteins are activated, undergo oligomerization, and localize to the mitochondrial outer membrane. The Bax and Bak activation causes mitochondrial outer membrane permeabilization, which allows the release of cytochrome c from the space between the two membranes. With the cooperation of apoptotic protease-activating factor 1(Apaf-1) and procaspase-9, the released cytochrome c forms the apoptosome complex. This complex can act as a platform for activating caspases. The apoptosome complex activates executive caspases, specifically caspases 3 and 7. These caspases are involved in executing the apoptotic process [3, 5]. By understanding the intrinsic apoptotic pathway, researchers can gain insights into the

* Corresponding author.
E-mail address: mparsania@iautmu.ac.ir (M. Parsania); frohollah@iautmu.ac.ir (F. Rouhollah) .
Doi: http://dx.doi.org/10.14715/cmb/2026.72.5.3

mechanisms of programmed cell death and develop targeted therapies for various diseases, including cancer.

Cancer treatments, like chemotherapy and radiation, are associated with side effects, and the main objective of many anti-cancer treatments is to reduce the rate of these side effects. Researchers are focusing on the development of anti-cancer drugs that direct cancer cells toward apoptosis [3]. In this regard, the use of complementary treatment methods, including medicinal plants, is expanding. Complementary therapies improve physical and emotional well-being, improve recovery from cancer and reduce the side effects of cancer treatment [6]**.** *Chelidonium majus* L. (*C. majus*) is widely distributed worldwide, including Asia, and is widely used in China against various diseases [7, 8]**.**

Different parts of this plant, including leaf, flower, and root extracts, are used to treat various diseases such as cancers. They have demonstrated cytotoxic effects on cancer cells by causing apoptosis. Cancers and cancer cells exhibiting sensitivity to the cytotoxic effects of *Chelidonium majus* L. and its primary alkaloid, chelidonine, include leukemia, PANC-1(pancreatic cancer), and HT-29 (colon cancer) cell lines [8]. *C.majus* L contains several alkaloid compounds such as chelidonine, chelerythrine, sanguinarine, berberine, protopine, allocryptopine, and coptisin, which have anti-cancer and anti-inflammatory impacts. These alkaloids have demonstrated significant antitumor activity in vivo and in vitro[9]. In traditional medicine, C.majus extract is used to treat warts caused by human papillomavirus (HPV) [10]. However, despite their advantages, the clinical applications of these secondary metabolites have been rarely used as complementary treatments due to their low solubility in water.

To address this issue, significant focus has been placed on various types of nanocarriers. These advancements lead to improved solubility of hydrophobic drugs, targeted drug delivery, controlled release, and enhanced drug efficacy [11]**.** Nanoparticles increase drug accumulation in a targeted manner in tumor tissue, thereby reducing the therapeutic dose of the drug and its side effects [11, 12]. Natural and synthetic polymers can serve as drug-delivery nanoparticles (NPs). Among these, human serum albumin (HSA) is of particular interest as a suitable candidate for drug delivery because of its excellent biocompatibility, non-toxicity, biodegradability, and non-immunogenicity [11]. Therefore, it can be postulated that the use of nanocarriers such as HAS-NPs can improve the drug delivery and efficacy of alkaloid compounds of C .majus in cancer treatment [13].

Although the anticancer effects of C. majus have been investigated in various cancer cells, there is a lack of reports comparing C. majus/AE and C. majus/HSA-NPs for targeted drug delivery to cancer cells and their anticancer activity. We compared the effects of C. majus/AE and C. majus/HSA on inducing internal apoptosis in HeLa cells.

2. Materials and methods

2.1. Preparation of *C. majus* alkaloid extract

The aerial parts (stem, leaves, flowers, and seeds) of Chelidonium majus were collected in May 2019 from the forest of Amol, northern Iran. The plant species was authenticated by experts from the Department of Pharmacognosy, Tehran Medical Sciences, Islamic Azad University (Voucher Specimen Code: 1630_AUPF). The plant material was dried at 25°C for 7 days and ground into a fine powder. The powdered material (100 g) was extracted three times with 500 mL of 80% methanol at room temperature for 24 h with intermittent shaking. The combined extract was filtered and concentrated under reduced pressure at 40°C. The concentrated extract was acidified to pH 2.0 with 1 N HCl and extracted with chloroform (3 × 100 mL) to remove non-alkaloid components. The aqueous layer was then basified to pH 10.0 with 1 N NaOH and extracted with chloroform (3 × 100 mL). The combined organic layers were dried over anhydrous Na_2SO_4 and evaporated to dryness to obtain the total alkaloid extract.

2.2. Synthesis of nanoparticles

Human serum albumin nanoparticles (HSA-NPs) and C. majus alkaloid extract-loaded HSA nanoparticles (C. majus/HSA-NPs) were prepared using the desolvation method with slight modifications [14, 15]. Briefly, 50 mg of HSA was dissolved in 1 mL of distilled water, and the pH was adjusted to 8.5 using 0.1 N NaOH. The alkaloid extract (10 mg) was dissolved in ethanol and added dropwise to the HSA solution under continuous stirring. Subsequently, 2 mL of ethanol was added as a desolvating agent at a flow rate of 1 mL/min under stirring at 700 rpm. To crosslink the nanoparticles, 50 µL of 8% glutaraldehyde was added, and the mixture was stirred for 2 h at room temperature. The resulting nanoparticles were purified by centrifugation at 15,000 rpm for 30 min, washed three times with distilled water, and lyophilized for further use. Unloaded HSA-NPs were prepared using the same procedure without the addition of the alkaloid extract.

The physicochemical properties of the nanoparticles were characterized using dynamic light scattering (DLS) and scanning electron microscopy (SEM) for particle size, morphology, and zeta potential. Fourier-transform infrared spectroscopy (FTIR) and X-ray diffraction (XRD) analyses were also performed to confirm nanoparticle formation and assess drug-polymer interactions. The nanoparticles exhibited a spherical morphology with diameters ranging from 200 to 300 nm. Encapsulation efficiency was determined indirectly by measuring the unencapsulated alkaloid content in the supernatant using UV-Vis spectroscopy at 280 nm. Detailed methodologies and comprehensive characterization datasets are presented in a concurrently published article from the same research project.

2.3. Cell lines

The HeLa cell line, derived from human cervical cancer, and a normal human fetal foreskin fibroblast cell line (HFFF-PI6), which represents normal cells, were sourced from the Pasteur Institute of Iran. Both cells were cultured in DMEM (Gibco, UK) treated with 100 IU/mL penicillin, 10% fetal bovine serum (FBS, Gibco, UK), and 100 µg/mL streptomycin (Gibco, UK). The cell lines were maintained at 37°C in an atmosphere containing 5% carbon dioxide.

2.4. MTT assay

Cell viability was assessed using the MTT (3-(4,5-dimethylthiazol-2-yl)-2,5-diphenyltetrazolium bromide) colorimetric assay. HeLa cells were seeded at a density of 2 × 10^4 cells per well in 96-well plates and incubated for 24 h to allow attachment. This seeding density was selected based on preliminary optimization experiments to ensure logarithmic cell growth during the treatment period. The

cells were then treated with various concentrations of *C. majus*/AE, *C. majus*/HSA-NPs, and HSA-NPs for 48 h. Specifically, *C. majus*/AE and *C. majus*/HSA-NPs were applied at concentrations of 10, 20, 30, 50, 100, 150, and 200 µg/mL, while HSA-NPs were tested at 100, 500, 1000, 1500, and 2000 µg/mL, as indicated on the x-axis of Figure 1a and 1b, respectively. Cells treated with equivalent volumes of the solvent (ethanol/PBS) served as vehicle controls, and untreated cells cultured in complete medium served as negative controls.

All treatments were performed in DMEM supplemented with 10% fetal bovine serum (FBS), 100 IU/mL penicillin, and 100 µg/mL streptomycin at 37°C in a 5% CO_2 atmosphere. After 48 h of incubation, the medium was carefully removed, and 20 µL of MTT reagent (5 mg/mL in phosphate-buffered saline, PBS) along with 80 µL of fresh RPMI medium were added to each well and incubated for an additional 4 h at 37°C. Subsequently, the supernatant was discarded, and 100 µL of dimethyl sulfoxide (DMSO) was added to each well to dissolve the formazan crystals. The optical density (OD) was measured at 560 nm using a microplate reader (Stat Fax 3200, USA). Blank wells containing 100 µL of DMSO without cells were used to subtract background absorbance.

The mean OD for each concentration was calculated from three replicate wells. The percentage of cytotoxicity was calculated using the following formula:

Cytotoxicity **(%)** = [1 − (Mean OD_{test} − Mean OD_{blank}) / (Mean $OD_{control}$ − Mean OD_{blank})] × 100

Viability **(%)** = 100 − Cytotoxicity (%)

The half-maximal inhibitory concentration (IC_{50}) was determined from the dose-response curve using non-linear regression analysis (GraphPad Prism version 9). All experiments were performed in triplicate and repeated at least three times independently.

2.5. Analysis of apoptosis by flow cytometry

Apoptosis was evaluated using the Annexin V-FITC Apoptosis Detection Kit (IQ Products, The Netherlands) according to the manufacturer's instructions. Following a 48-hour treatment period, both adherent and floating cells were carefully collected, pooled, and washed twice with ice-cold PBS to ensure the inclusion of all apoptotic and detached cell populations. The cell pellets were resuspended in 100 µL of binding buffer containing 5 µL of Annexin V-FITC and 5 µL of propidium iodide (PI), and incubated for 15 min at room temperature in the dark. After incubation, 400 µL of binding buffer was added to each sample, and the cells were immediately analyzed using a BD FACS Calibur flow cytometer (BD Biosciences, San Jose, CA, USA). For each sample, at least 10,000 **events** were acquired. The gating strategy was established based on forward scatter (FSC) versus side scatter (SSC) to exclude cell debris and doublets. Quadrant gates were set using unstained cells, single-stained Annexin V-FITC controls, and single-stained PI controls to discriminate between viable cells (Annexin V^-/PI^-), early apoptotic cells (Annexin V^+/PI^-), late apoptotic/necrotic cells (Annexin V^+/PI^+), and necrotic cells (Annexin V^-/PI^+). Data analysis was performed using FlowJo 10 software.

To evaluate the dose-dependent apoptotic effect, HeLa cells were treated with sub-cytotoxic, IC_{50}, and supra-cytotoxic concentrations of the extracts. Specifically, C. majus/AE was applied at 50 µg/mL (sub-IC_{50}), 70.79 µg/mL (IC_{50}), and 150 µg/mL (supra-IC_{50}), while C. majus/HSA-NPs were applied at 30 µg/mL (sub-IC_{50}), 52.37 µg/mL (IC_{50}), and 100 µg/mL (supra-IC_{50}). Unloaded HSA-NPs were tested at 50 and 100 µg/mL to assess their intrinsic effect on apoptosis. For fibroblast cells, to evaluate the safety profile of the treatments, concentrations of 50, 100, and 150 µg/mL were selected for both C. majus/AE and C. majus/HSA-NPs, as these doses corresponded to the effective range in cancer cells while remaining well below the fibroblast IC_{50} values (>750 µg/mL). Untreated cells served as negative controls.

It is important to note that while real-time PCR analysis was performed exclusively at the IC_{50} concentration to investigate the molecular signaling pathways specifically engaged at the half-maximal inhibitory dose, flow cytometry was conducted across a broader range of concentrations (sub-IC_{50}, IC_{50}, and supra-IC_{50}). This experimental design was intentionally implemented to comprehensively evaluate the dose-dependent progression of apoptotic cell death, thereby providing both mechanistic insights (via gene expression at IC_{50}) and pharmacological dose-response characterization (via flow cytometry across multiple doses). All experiments were performed in triplicate and repeated independently at least three times.

2.6. RNA extraction and real-time PCR

Total RNA from HeLa cells and fibroblasts treated at IC50 concentrations with *C. majus*/AE, *C. majus*/HSA-NPs (IC50 70.79 and 52.37 µg/ml, respectively) using the RNA extraction kit of Yekta Tajhiz Azma(YTA), as instructed. cDNA strand was produced from RNA using a reverse transcription system with a random hexamer primer as instructed (Yekta Tajhiz Azma (YTA)). *Caspase-3*, *caspase-9*, *Bax*, and *Bcl2* RNA expression levels were measured by RT-PCR using SYBR Green PCR Master Mix (YTA).

Table 1 lists the primers used. CT values for target genes and GAPDH were measured for all samples, and the target genes' expression levels were normalized against GAPDH expression. PCR amplification was done in a 20 µL reaction volume including 8 µL of PCR-grade water, 0.5 µL of primers, 10 µL SYBR Green PCR Master Mix, and 1 µL of cDNA. The reactions were conducted with a primary denaturation at 95˚C for 10 minutes, and then 40 cycles of denaturation (95˚C / 30 seconds), annealing (56˚C / 30 seconds), and extension (72˚C / 30 seconds). Additionally, the melting curve (68 ℃/95 ℃) was monitored. The RT-PCR program was consistent across all genes. Each test included a negative control. RT-PCR was done using the LightCycler® 96 Instrument (Roche Molecular Systems, Germany). The relative quantity was calculated according to $2^{-\Delta\Delta Cq}$ method.

2.7. Statistical Analysis

Statistical analyses were performed using SPSS version 25 (IBM Corp., Armonk, NY, USA). Data are presented as mean ± standard deviation (SD) from three independent experiments, each performed in triplicate. The normality of data was assessed using the Shapiro-Wilk test. Differences between two groups were analyzed using the unpaired two-tailed Student's t-test. For comparisons of more than two groups, one-way analysis of variance (ANOVA) was used, followed by Tukey's post hoc test for multiple comparisons. Gene expression differences were assessed

Table 1. Specifications of primers applied for PCR.

Gene	Primer sequence 5'--3'	Product length (bp)
Bax	F: GAT GCG TCC ACC AAG AA R: AGT TGA AGT TGC CGT CAG	163
Bcl2	F:CAT CAG GAA GGC TAG AGT TA R:CAG ACA TTC GGA GAC CAC AC	181
Caspase 3	F:TTC AGA GGG GAT CGT TGT AGA AGT C R:CAA GCT TGT CGG CAT ACT GTT TCA G	264
Caspase 9	F:ATT GTT GAT AAT GAG GCA GTG G R:GGT GAT GTC GGT GCT CTT G	96
GAPDH	F:CTC TTG CTA CTC TGC TCT G R:GCC TGC CTG GTG ATA ATC	179

using GenEx 6 software. Graphs were created using GraphPad Prism version 9. A p-value < 0.05 was considered statistically significant (*p* < 0.05, **p* < 0.01, ***p* < 0.001, ****p* < 0.0001).

3. Results

3.1. Cellular cytotoxicity

After exposing HeLa cells to extracts for 48 hours, we observed cytotoxic effects that were associated with the extracts' concentration. The IC50 values were measured as 70.79 µg/mL, 52.37 µg/mL, and greater than 2000 µg/mL for *C. majus*/AE, *C. majus*/HSA-NPs, and HSA-NPs, respectively, after 48 hours. The cytotoxic effects of the extracts on fibroblast cells were assessed, revealing the IC50 values. The IC50 for *C. majus*/AE was found to be 835 µg/mL, whereas the values for C. majus/HSA-NPs and HSA-NPs exceeded 1600 µg/mL after 48 hours.

Figure 1 displays the viability of HeLa cells receiving varying concentrations of C. majus extract (C. majus/AE)

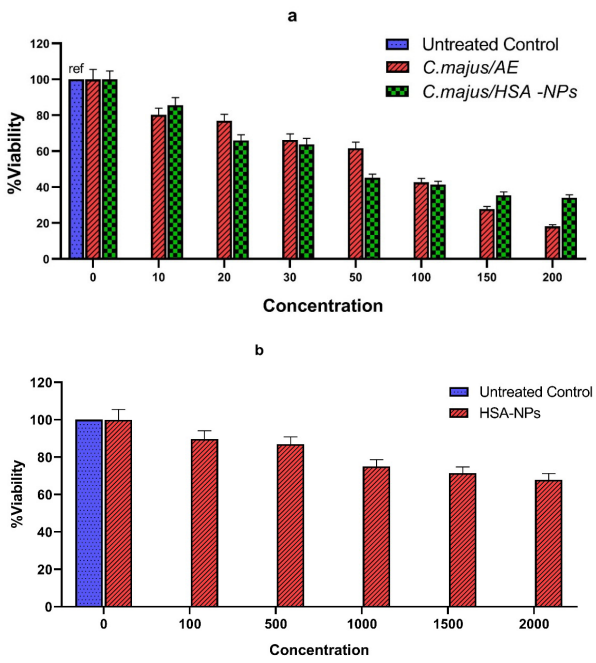


Fig. 1. Viability of HeLa cells by MTT assay in the treatment; a: *C. majus*/AE and *C. majus*/HSA -NPs at 10-20-30-50-100-150-200 µg/mL concentrations, b: HSA-NPs at 100-500-1000-1500-2000 µg/mL concentrations. The mean percentage of viability of three separate experiments is illustrated in this graph.

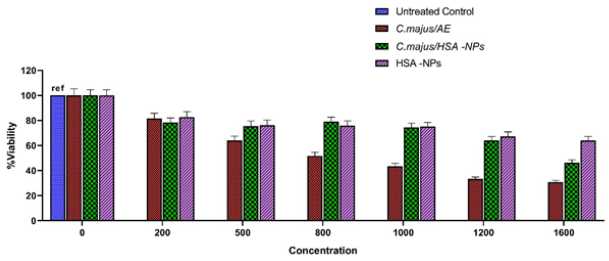


Fig. 2. The effect of *C. majus*/AE, *C. majus*/ HSA-NPs, and HSA-NPs on fibroblast cells was investigated using the MTT assay. The cells received extract at 200, 500, 800, 1000, 1200, and 1600 µg/mL for 48 hours. The mean percentage of viability of the three separate experiments is shown in this graph.

and C. majus/HSA nanoparticles (C. majus/HSA-NPs). The results indicate that cell viability was dose-dependent, with a reduction observed at 10 µg/mL to 200 µg/mL concentrations after 48 hours (Panel a). In Graph b, treating HeLa cells with different concentrations of HSA-NPs shows that up to 2000 µg/mL, 75% of the cells survived. Additionally, Figure 2 illustrates the cytotoxic effects of C. majus/AE, C. majus/HSA-NPs, and HSA-NPs on fibroblast cells.

3.2. Apoptotic activity of *C. majus*/AE and *C. majus*/HSA-NPs

Flow cytometry results indicated that 35.2% of HeLa cells treated with 70.79 µg/mL (IC50) C. majus/AE underwent apoptosis, with 22.9% in early stages and 12.3% in late stages (Fig. 3b). Also, the results showed that the *C. majus*/AE at a higher IC50 (150 µg/ml) 40.6% (13.7% of late apoptosis and 26.9% of early apoptosis) compared to the extract's sub-toxic concentration (50 µg/ml)19.89% (11.2% early apoptosis and 8.69% late apoptosis) led to cell death (Fig 3b).

The results obtained by flow cytometry in *C.majus*/HSA-NPs cells, in HeLa cells also demonstrated similar results to *C. majus*/AE, where IC50 (52.37 µg/ml) resulted in 40.5% apoptosis (22.3% late apoptosis and 17.2% early apoptosis) compared to subtoxic concentration (30 µg/mL) 40.2% apoptosis(27.2% late apoptosis and 13% early apoptosis) (Fig. 3b). *C.majus*/AE at a higher IC50 (100 µg/mL) caused 46.9% cell death, comprising 23.9% early apoptosis and 23% late apoptosis (Fig 3b).

Flow cytometry analysis demonstrated that treatment of cells with 50 and 100 µg/mL concentrations of HSA-

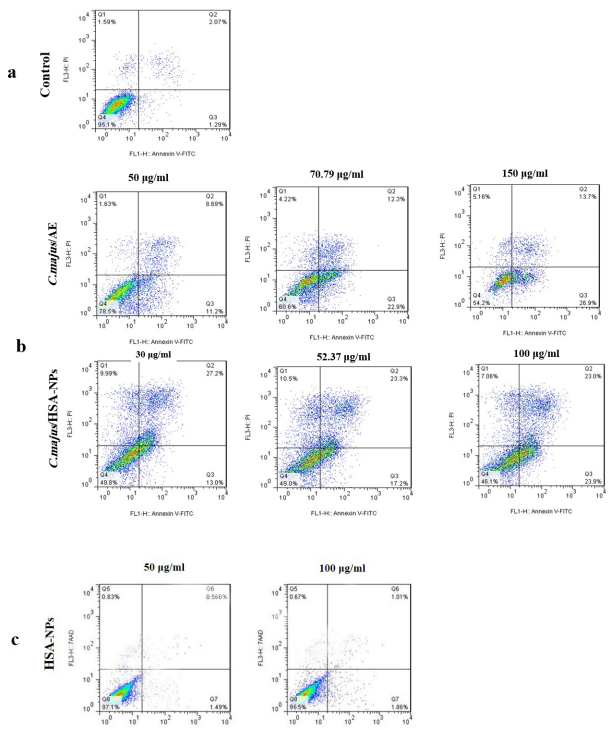


Fig. 3. Flow cytometry plot of Annexin/PI test. Chart of the number of living cells, late and early apoptosis, and necrosis. HeLa cells (a): untreated as control, (b): treated with *C. majus*/AE (50- 70.79- 150 µg/ml) and *C. majus*/ HSA-NPs (30-52.37-100µg/ml), (c): treated with HSA-NPs at a concentration of 50-100 µg/mL for 48 hours.

NPs resulted in over 96% cell viability, indicating minimal cytotoxic effects at these doses (Fig. 3c).

We also evaluated the apoptotic cell death of *C. majus*/AE, *C. majus*/HSA-NPs, and HSA-NPs in fibroblast cells using the same method. This study showed that *C. majus*/AE, *C. majus*/HSA-NPs, and HSA-NPs in fibroblasts did not affect normal cells and did not lead to apoptosis compared to approximately similar concentrations in HeLa cells (50-100-150 µg/m (Fig. 4).

3.3. Gene expression using RT- PCR

Caspase 3-9, Bax, and *Bcl2* expression was investigated by RT- PCR. Their expression was measured after receiving IC50 concentrations of *C. majus*/AE and *C. majus*/HSA-NPs in the HeLa cells.

The caspase-3 and caspase-9 mRNA levels in HeLa cells increased 7.7-fold and 4.08-fold, respectively, after treatment at the IC50 of *C. majus*/AE in comparison to the controls, which had a 1-fold change ($p<0.05$). Similarly, the *caspase-3* and *caspase-9* mRNA levels in the HeLa cells after receiving *C. majus*/HSA-NPs at IC50 were significantly increased by 181.6-fold and 21.5-fold, respectively, in comparison to the controls ($p<0.0001$) (Fig. 5).

The findings showed that *C.majus*/AE and *C.majus*/HSA-NPs treatment caused a significant concentration-dependent elevation in the mRNA levels of *Bax* and a concomitant reduction in the level of the anti-apoptotic protein Bcl2, thereby increasing the ratio *Bax/Bcl2* that promoted apoptosis. Specifically, the *Bax* mRNA levels showed an increase of about 9.98-fold ($P<0.05$) and 11.47-fold ($P<0.05$) for *C. majus*/AE and *C. majus*/HSA-NPs treatment at IC50, respectively, in comparison to the untreated controls. However, after 48 hours of exposure to *C. majus*/AE and *C. majus*/HSA-NPs, the ratio of *Bcl2* at IC50 concentrations decreased significantly ($P<0.05$). At the IC50 concentrations, the *Bax/Bcl-2* ratio significantly enhanced to 14.71 and 19.65 in cells treated with *C. majus*/AE and *C. majus*/HSA-NPs, respectively, indicating enhanced pro-apoptotic signaling ($P<0.05$). Thus, the Bax/Bcl2 ratio was significantly increased by treatment with *C.majus*/HSA-NPs compared to *C.majus*. Finally, there was a significant relationship between the concentrations of *C. majus*/AE and *C. majus*/HSA-NPs (Fig. 6).

MTT assay results indicated that treatment with *C. majus*/AE, *C. majus*/HAS, and HSA-NPs had no significant cytotoxic effect on normal fibroblast cells, as cell viability remained above 90% across all tested concentrations. Due

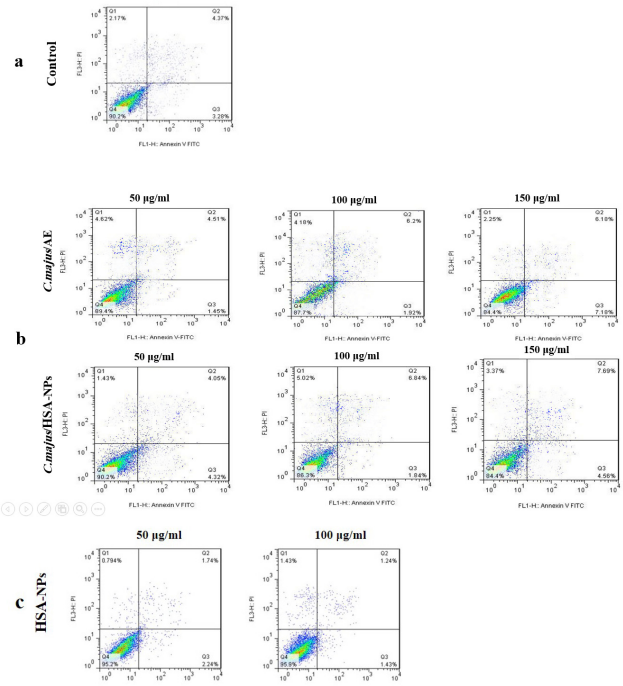


Fig. 4. Annexin/PI test flow cytometry diagram. A graph of the number of viable cells, late and early apoptosis, as well as necrosis. Fibroblast cells (a): untreated as control, (b): treated with *C.majus*/AE (50-100-150 µg/mL) and *C.majus*/HSA-NPs (50-100-150 µg/mL), (c): treated with HSA-NPs at 50-100 µg/mL for 48 hours.

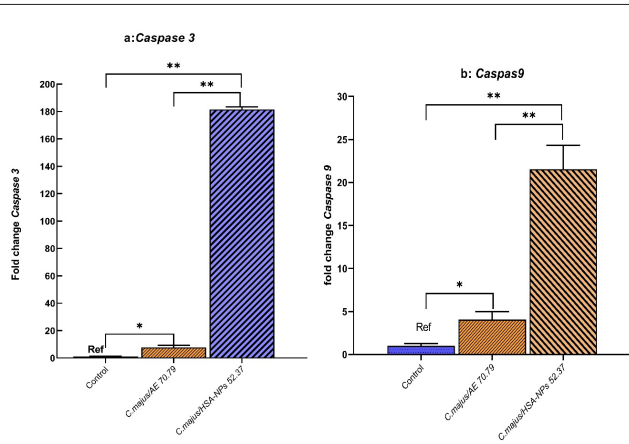


Fig. 5. Expression of caspase-3 (a) and caspase-9 (b) genes in HeLa cells after 48 hours of treatment with *C.majus*/AE and *C.majus*/HSA-NPs. Significant *Caspase-3* and *Caspase-9* expression at the IC50 concentration versus the controls was observed (*p <0.05, **p <0.0001).

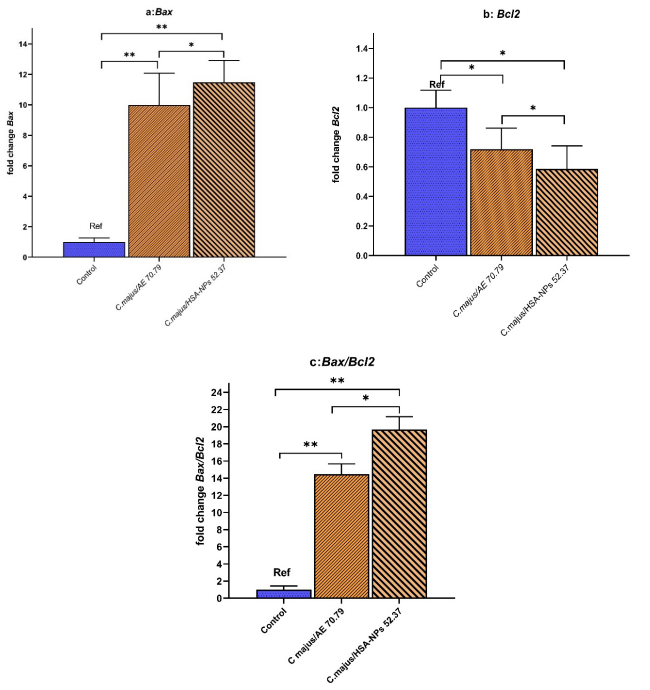


Fig. 6. Expression of *Bax* (a), *Bcl2* (b), and ratio Bax/Bcl2 (c) genes in HeLa cell lines following 48 hours of treatment with *C majus*/AE, *C.majus*/HSA-NPs at IC50. There was a significant elevation in the expression of *Bax* and *Bcl2* genes and the ratio *Bax/Bcl2* at IC50 concentration versus the controls (*p < 0.05, **p-value < 0.0001). The association between *C. majus*/AE and *C. majus*/HSA-NPs was significant.

to the absence of any significant reduction in cell viability or morphological changes in fibroblasts, real-time PCR analysis was not performed for this cell line. The gene expression studies were therefore focused solely on the HeLa cancer cells.

4. Discussion

Cervical cancer is a significant global health challenge, especially in areas with limited access to advanced healthcare services. Traditional treatment options, such as chemotherapy and radiation therapy, often lead to substantial toxicity and the risk of developing drug resistance. These issues underscore the urgent need for innovative therapeutic strategies that minimize side effects while improving treatment effectiveness. Natural anti-cancer compounds, particularly plant-derived alkaloids, have demonstrated considerable potential as effective inducers of apoptosis, which is a critical mechanism in cancer treatment [16].

We evaluated the effect of human serum albumin nanoparticles as an alkaloid extract delivery system to trigger HeLa cell apoptosis. *C. majus* extracts exhibited concentration-dependent cytotoxicity, both for *C. majus/AE* and *C. majus*/HSA-NPs formulations. This was shown by the upregulation of pro-apoptotic gene expression, including caspases 3 and 9, along with an elevation in *Bax* expression and a reduction in *Bcl-2* levels, ultimately triggering apoptosis in cancer cell lines without impacting fibroblasts.

Research on *Chelidonium majus* L. has predominantly focused on its ethanolic, aqueous, and alkaloid extracts, as well as specific compounds such as berberine and sanguinarine. These extracts have demonstrated many biological activities, including anti-inflammatory, cytotoxic and antimicrobial effects against various cell lines [16, 17]. Our study compared the efficacy of C. majus/HSA-NPs and C. majus/AE in inducing intrinsic apoptosis in HeLa cells.

Studies investigating the cytotoxic and antitumor effects of *Chelidonium majus* L. ethanolic extract on various cancer cells, including MDA-MB-231, HCT 116, A549, SW480, H460, and MCF-7, have demonstrated significant cytotoxic activities. For example, treatment of A549 cells with the crude extract decreased Bcl2 expression while simultaneously increasing the *Bax and caspase-3* expression. Similarly, the aqueous extract of *Chelidonium majus* L. showed marked anti-proliferative activity against MCF-7 cells, which can be attributed to the alkaloid chelerythrine [16, 17].

Targeting apoptosis has become a promising non-surgical approach in cancer treatment, given that the ability to evade apoptosis is a defining characteristic of cancer cells. Numerous anticancer drugs have been developed to target different steps within the intrinsic and extrinsic apoptotic pathways [5]. Unlike necrosis, apoptosis is a highly programmed and regulated process that minimizes damage to surrounding cells.

Therefore, induction of apoptosis represents a promising therapeutic strategy for cancer treatment. In the intrinsic (mitochondrial) apoptotic pathway, Bax and Bcl-2 are key regulatory proteins, and the Bax/Bcl-2 ratio is a critical determinant of cellular susceptibility to apoptosis [18]. Accordingly, investigating the effects of *C. majus* and its HSA nanoparticle formulation on these apoptotic regulators may provide valuable insights into their underlying anticancer mechanisms.

While alkaloids such as berberine and sanguinarine show potent antitumor and anticancer properties, their clinical use is often limited by unfavorable physicochemical characteristics such as low solubility, poor stability, and limited bioavailability. To address these limitations, nanoparticle-oriented delivery systems have been developed to increase the pharmacokinetic and physicochemical properties of alkaloids, thereby improving their therapeutic potential [19].

Notably, nanoparticles utilizing human serum albumin as a carrier have demonstrated promising efficacy in cancer therapy. The incorporation of drugs with HSA nanoparticles mitigates drug resistance, while the high biocompatibility of albumin minimizes immune responses and toxicity. In vitro studies have shown that HSA-based nanoparticles significantly improve the cytotoxicity of drugs compared to non-nanoparticle formulations, making them promising candidates for targeted cancer therapy [14, 16, 20].

This research utilized MTT and flow cytometry assays to evaluate the cytotoxic and apoptosis-inducing effects of *C. majus*/AE and *C. majus*/HSA-NPs on HeLa cells. Both formulations displayed concentration-dependent anti-proliferative and apoptosis-inducing activities. Notably, *C. majus*/HSA-NPs induced apoptosis at lower concentrations than *C. majus*/AE, demonstrating superior efficacy. These findings highlight the potential of *C. majus*/HSA-NPs as a more effective candidate for anticancer therapy compared to the crude alkaloid extract.

Paul et al. examined the effects of free chelidonin (FC) and chelidonin encapsulated in PLGA nanoparticles (NC) on HepG2 liver cancer cells. Both formulations upregulated the *Bax* and *caspase-3* expression, but the NC formulation showed superior efficacy, significantly increasing

Bax, *caspase-9*, and *caspase-3* levels compared to the free chelidonin [21].

Similarly, our study demonstrated that treatment with *C. majus*/HSA-NPs and *C. majus*/AE both led to the upregulation of *Bax* expression, thereby enhancing apoptosis compared to the control groups. Notably, ***C. majus***/HSA-NPs induced apoptosis more effectively than *C. majus*/AE at lower doses, reinforcing their potential as superior therapeutic agents for cancer treatment.

The apoptotic effects of alkaloids such as berberine and sanguinarine have been widely documented. For example, berberine has been shown to increase *Bax* expression and decrease *Bcl2* levels in various cancer cell lines, including breast cancer, oral squamous cell carcinoma, and CC [22, 23]. In the HL-60/MX2 hematopoietic cancer cell line, berberine was found to increase *Bax* expression while decreasing *Bcl2* levels, thereby promoting apoptosis [6, 11, 13, 21, 24]. Furthermore, berberine exhibited pro-apoptotic and anti-proliferative effects in HeLa cell lines and patients with B-cell chronic lymphocytic leukemia (B-CLL) by enhancing Bax expression and activating ***caspase-3*** [18, 22, 25, 26]. It has been reported that berberine increased the *Bax/Bcl2* ratio and facilitated the cytochrome c release from mitochondria in HeLa cells, thereby triggering mitochondrial apoptosis [18, 26, 27].

Similarly, Adhami et al. assessed the effects of sanguinarine on immortal human keratinocyte cells (HaCaT cells). They observed a dose-dependent increase in *Bax* levels accompanied by a decrease in *Bcl2* levels, which elevated the *Bax/Bcl2* ratio and promoted apoptosis. Thus, sanguinarine treatment can induce apoptosis in HaCaT cells by modulating the levels of *Bax* and *Bcl2,* highlighting its potential as a therapeutic agent for targeting abnormal cell growth [28]. The present study demonstrates that treatment with *C.majus*/HSA-NPs significantly enhanced the *Bax/Bcl2* ratio compared to *C. majus*/AE alone. Both *C. majus*/AE and *C. majus*/HSA-NPs effectively upregulated the expression of the *Bax* pro-apoptotic gene, resulting in an elevated *Bax/Bcl2* ratio. These findings underscore the potential of *C. majus*/HSA-NPs as a promising anticancer agent due to their ability to modulate apoptotic pathways and promote apoptosis in HeLa cells. Additionally, the research comprehensively examined the effects of the alkaloid extract and its constituents on the expression of apoptotic markers, like *Bax*, *Bcl2*, and *caspases 3* and *9*. This detailed analysis further underscores the therapeutic potential of *C. majus*/HSA-NPs in cancer therapy by enhancing the expression of key apoptotic regulators and effectively modulating intrinsic apoptotic pathways.

In line with previous research on alkaloids, studies by Binan Lu have demonstrated that berberine exhibits significant anti-proliferative effects on human cervical carcinoma HeLa cells. Specifically, berberine treatment markedly enhanced the activity of *caspase-3,* an important executor of apoptosis [18]. Further investigation into the effects of berberine on additional cervical cancer cell lines, SiHa and Ca Ski, revealed that berberine treatment upregulated *Bax* expression while downregulating Bcl2 expression, thereby activating caspases, including *caspase-3,* further promoting apoptosis [29].

Additionally, Wang et al. investigated the anti-tumor impacts of berberine on human liver cancer cells, including HepG2 and MHCC97 L. Berberine induced apoptosis in hepatocellular carcinoma cells by upregulating *Bax* expression, facilitating the cytochrome c release into the cytosol, and activating *caspases 3* and *9.* Specifically, berberine triggers mitochondrial apoptosis in HCC cells through *Bax*-mediated cytochrome c release and activating the caspase-3 and caspase-9 signaling pathways [30].

Both sanguinarine and berberine induce apoptosis in hematopoietic cancer cell lines via the mitochondrial apoptotic pathway. These compounds exhibit significant cytotoxic and pro-apoptotic activities, underscoring their potential as candidates for anti-cancer therapy. The mitochondrial apoptotic pathway is mediated by the pro-apoptotic ***Bcl2*** *family member BID, ultimately causing the activation of caspase 3* and *caspase 9* [24].

A study investigating the effects of sanguinarine on apoptosis in human keratinocyte cells (HaCaT) revealed that treatment with sanguinarine was dose-dependent and led to increased protein expression of *caspases 3, 7, 8,* and *9* [28].

Compounds such as berberine, sanguinarine, and chelidonine are notable alkaloids found in the extract of *C. majus.* Our findings align with previous research on these alkaloids, highlighting their critical role in the biological activity of this plant extract. Specifically, these compounds demonstrate many pharmacological effects, including significant anticancer properties, which further validates the consistency of our results with earlier studies.

The *caspase-3* and *caspase-9* expression levels dose-dependently increased following treatment with *C. majus*/AE and *C. majus*/HSA-NPs. This suggests that the activation of apoptotic pathways in response to these treatments with higher concentrations may enhance apoptotic signaling through these caspases. These findings highlight the critical role of dosage in modulating apoptotic gene expression, which can inform therapeutic strategies targeting apoptosis in various diseases.

The findings also indicated that C. majus/HSA-NPs showed significant apoptotic potential, suggesting their use as a supplementary therapeutic agent in cervical cancer chemotherapy. However, further comprehensive studies should validate these preliminary results and elucidate the underlying mechanisms of action. Continued research in this field is essential to optimize therapeutic strategies and improve treatment outcomes for cervical cancer. Importantly, our study highlights the selective toxicity of *C. majus*/HSA-NPs toward cancer cells, as demonstrated by the absence of significant apoptotic effects on normal fibroblast cells. While this study showed encouraging results, several limitations need to be addressed. Although laboratory experiments on HeLa cells were performed, further investigations using animals and human clinical trials are required to confirm these results. Furthermore, translational research should seek to clarify the precise biological mechanisms that *C. majus*/HSA-NPs activate to induce apoptosis, while also considering other relevant signaling responses. An evaluation of nanoparticle stability and formulation toxicity is crucial for safe clinical application.

5. Conclusion

This research demonstrated that *C. majus*/HSA-NPs induced significant cytotoxicity and pro-apoptotic effects in HeLa cells that surpass the performance of crude extract. The nanoparticle formulation upregulated apoptotic marker expression of *caspase-3* and *caspase-9* as well as

Bax while downregulating *Bcl2*, thereby demonstrating higher apoptosis potential in cancer cells. *C. majus*/HSA-NPs demonstrated selective antitumor effects that protect healthy fibroblasts from cell death. *C. majus*/HSA-NPs demonstrated therapeutic potential for cervical cancer as an advanced targeted agent that yields improved outcomes while reducing the typical side effects associated with current treatments. Future research should assess the specific clinical applications of this medication formulation and confirm its operational mechanisms through more thorough analysis.

There were no concerns regarding the immunogenicity of these nanoparticles because human serum albumin, the most abundant protein in human plasma, was used. However, further investigation of in vivo animal models is needed to confirm this. The combination of plant-derived nanoparticles, such as those from *C. majus*/ HSA-NPs, has shown promising results in preclinical studies for cancer treatment.

Abbreviations

C. majus, Chelidonium majus L.; NPs, nanoparticles; HSA-NPs, human serum albumin nanoparticles; C. majus/AE, C. majus alkaloid extract; C. majus/HSA-NPs, nanoformulation of C. majus alkaloid extract; RT-PCR, real-time reverse transcription polymerase chain reaction; Apaf-1, apoptotic protease-activating factor 1; HPV, human papillomavirus; HSA, human serum albumin; IC₅₀, half-maximal inhibitory concentration; CC, cervical cancer; Bax, BCL2-associated X protein; Bcl-2, B-cell lymphoma 2 protein; Bak, BCL2 antagonist/killer 1; GAPDH, glyceraldehyde-3-phosphate dehydrogenase; FC, free chelidonine; PLGA, poly(lactic-co-glycolic acid); B-CLL, B-cell chronic lymphocytic leukemia.

Acknowledgments

The authors wish to extend their profound appreciation to the late Professor Dr. Gholamreza Amin for his exceptional scientific contributions to this work. His expertise in the accurate identification of the plant species and his meticulous preparation of the plant extract were essential to the progress and completion of this research project. His contributions are gratefully acknowledged. We would like to thank the staff of the Medical Genomics Research Center, Tehran Medical Sciences Islamic Azad University, Tehran, Iran.

Conflicts of Interest

The authors declare no conflicts of interest related to this research.

Competing Interests

The authors declare no conflicts of interest, financial or otherwise, relevant to the content of this work.

Author Contributions

All authors contributed to the conception and design of the study. Material preparation, data collection, and data analysis were conducted by Mahdieh Imani, Masoud Parsania, Fatemeh Rouhollah and Mohammad Hassan Pouriayevali. The initial manuscript draft was prepared by Mahdieh Imani, and all authors critically reviewed and provided feedback on subsequent versions. All authors have read and approved the final version of the manuscript.

Ethical Approval and Consent to Participate

This study received ethical approval from the Research Ethics Committee of Tehran Islamic Azad Medical Sciences University (Approval Code: IR.IAU.PS.REC.1398.261).

Funding

The authors did not receive support from any organization for the submitted work. The authors have no financial or proprietary interests in any material discussed in this article.

Data Availability

The datasets generated and/or analyzed during the current study are available from the corresponding author upon reasonable request.

Use of Artificial Intelligence Tools

Some sentences in this manuscript were revised with the assistance of artificial intelligence, using language models to improve clarity and readability. All intellectual content, interpretations, and conclusions are solely the responsibility of the authors.

References

1. Crippin T, Tounkara K, Munir H, Squibb E, Piotrowski C, Koita OA, Teguété I, De Groot AS (2024) Our Daughters-Ourselves: Evaluating the Impact of Paired Cervical Cancer Screening of Mothers with HPV Vaccination for Daughters to Improve HPV Vaccine Coverage in Bamako, Mali. Vaccines (Basel) 12 (9). doi: 10.3390/vaccines12091019
2. Arjomandnejad M, Muhammadnejad A, Haddadi M, Sherkat-Khameneh N, Rismanchi S, Amanpour S, Muhammadnejad S (2014) HeLa cell line xenograft tumor as a suitable cervical cancer model: growth kinetic characterization and immunohistochemistry array. Arch Iran Med 17 (4): 273-277. doi:
3. Yuan CH, Filippova M, Duerksen-Hughes P (2012) Modulation of apoptotic pathways by human papillomaviruses (HPV): mechanisms and implications for therapy. Viruses 4 (12): 3831-3850. doi: 10.3390/v4123831
4. Favaloro B, Allocati N, Graziano V, Di Ilio C, De Laurenzi V (2012) Role of apoptosis in disease. Aging (Albany NY) 4 (5): 330-349. doi: 10.18632/aging.100459
5. 5. Pfeffer CM, Singh ATK (2018) Apoptosis: A Target for Anticancer Therapy. Int J Mol Sci 19 (2). doi: 10.3390/ijms19020448
6. Kooti W, Servatyari K, Behzadifar M, Asadi-Samani M, Sadeghi F, Nouri B, Zare Marzouni H (2017) Effective Medicinal Plant in Cancer Treatment, Part 2: Review Study. J Evid Based Complementary Altern Med 22 (4): 982-995. doi: 10.1177/2156587217696927
7. Samatadze TE, Yurkevich OY, Hazieva FM, Konyaeva EA, Morozov AI, Zoshchuk SA, Amosova AV, Muravenko OV (2020) Agro-Morphological, Microanatomical and Molecular Cytogenetic Characterization of the Medicinal Plant Chelidonium majus L. Plants (Basel) 9 (10). doi: 10.3390/plants9101396
8. Terzic M, Fayez S, Fahmy NM, Eldahshan OA, Uba AI, Ponniya SKM, Selvi S, Nilofar, Koyuncu I, Yüksekdağ Ö, Zengin G (2024) Chemical characterization of three different extracts obtained from Chelidonium majus L. (Greater celandine) with insights into their in vitro, in silico and network pharmacological properties. Fitoterapia 174: 105835. doi: 10.1016/j.fitote.2024.105835
9. Noureini SK, Esmaeili H, Abachi F, Khiali S, Islam B, Kuta M, Saboury AA, Hoffmann M, Sponer J, Parkinson G, Haider S (2017) Selectivity of major isoquinoline alkaloids from Cheli-

donium majus towards telomeric G-quadruplex: A study using a transition-FRET (t-FRET) assay. Biochim Biophys Acta Gen Subj 1861 (8): 2020-2030. doi: 10.1016/j.bbagen.2017.05.002
10. Nawrot R, Warowicka A, Rudzki PJ, Musidlak O, Dolata KM, Musijowski J, Stolarczyk EU, Goździcka-Józefiak A (2021) Combined Protein and Alkaloid Research of Chelidonium majus Latex Reveals CmMLP1 Accompanied by Alkaloids with Cytotoxic Potential to Human Cervical Carcinoma Cells. Int J Mol Sci 22 (21). doi: 10.3390/ijms222111838
11. Qu N, Sun Y, Li Y, Hao F, Qiu P, Teng L, Xie J, Gao Y (2019) Docetaxel-loaded human serum albumin (HSA) nanoparticles: synthesis, characterization, and evaluation. Biomed Eng Online 18 (1): 11. doi: 10.1186/s12938-019-0624-7
12. S MS, Naveen NR, Rao GK, Gopan G, Chopra H, Park MN, Alshahrani MM, Jose J, Emran TB, Kim B (2022) A spotlight on alkaloid nanoformulations for the treatment of lung cancer. Front Oncol 12: 994155. doi: 10.3389/fonc.2022.994155
13. Lomis N, Westfall S, Farahdel L, Malhotra M, Shum-Tim D, Prakash S (2016) Human Serum Albumin Nanoparticles for Use in Cancer Drug Delivery: Process Optimization and In Vitro Characterization. Nanomaterials (Basel) 6 (6). doi: 10.3390/nano6060116
14. Sebak S, Mirzaei M, Malhotra M, Kulamarva A, Prakash S (2010) Human serum albumin nanoparticles as an efficient noscapine drug delivery system for potential use in breast cancer: preparation and in vitro analysis. Int J Nanomedicine 5: 525-532. doi: 10.2147/ijn.s10443
15. Lin W, Garnett MC, Davis SS, Schacht E, Ferruti P, Illum L (2001) Preparation and characterisation of rose Bengal-loaded surface-modified albumin nanoparticles. J Control Release 71 (1): 117-126. doi: 10.1016/s0168-3659(01)00209-7
16. Yurt F, Özel D, Tunçel A, Gokbayrak O, Aktas S (2023) Synthesis and Optimization of the Docetaxel-Loaded and Durvalumab-Targeted Human Serum Albumin Nanoparticles, In Vitro Characterization on Triple-Negative Breast Cancer Cells. ACS Omega 8 (29): 26287-26300. doi: 10.1021/acsomega.3c02682
17. Deljanin M, Nikolic M, Baskic D, Todorovic D, Djurdjevic P, Zaric M, Stankovic M, Todorovic M, Avramovic D, Popovic S (2016) Chelidonium majus crude extract inhibits migration and induces cell cycle arrest and apoptosis in tumor cell lines. J Ethnopharmacol 190: 362-371. doi: 10.1016/j.jep.2016.06.056
18. Lu B, Hu M, Liu K, Peng J (2010) Cytotoxicity of berberine on human cervical carcinoma HeLa cells through mitochondria, death receptor and MAPK pathways, and in-silico drug-target prediction. Toxicol In Vitro 24 (6): 1482-1490. doi: 10.1016/j.tiv.2010.07.017
19. Zheng X, Wu F, Lin X, Shen L, Feng Y (2018) Developments in drug delivery of bioactive alkaloids derived from traditional Chinese medicine. Drug Deliv 25 (1): 398-416. doi: 10.1080/10717544.2018.1431980
20. Saleh T, Soudi T, Shojaosadati SA (2019) Aptamer functionalized curcumin-loaded human serum albumin (HSA) nanoparticles for targeted delivery to HER-2 positive breast cancer cells. Int J Biol Macromol 130: 109-116. doi: 10.1016/j.ijbiomac.2019.02.129
21. Paul A, Das S, Das J, Samadder A, Khuda-Bukhsh AR (2013) Cytotoxicity and apoptotic signalling cascade induced by chelidonine-loaded PLGA nanoparticles in HepG2 cells in vitro and bioavailability of nano-chelidonine in mice in vivo. Toxicol Lett 222 (1): 10-22. doi: 10.1016/j.toxlet.2013.07.006
22. Li Q, Zhao H, Chen W, Huang P (2023) Berberine induces apoptosis and arrests the cell cycle in multiple cancer cell lines. Arch Med Sci 19 (5): 1530-1537. doi: 10.5114/aoms/132969
23. Och A, Och M, Nowak R, Podgórska D, Podgórski R (2022) Berberine, a Herbal Metabolite in the Metabolic Syndrome: The Risk Factors, Course, and Consequences of the Disease. Molecules 27 (4). doi: 10.3390/molecules27041351
24. Och A, Zalewski D, Komsta Ł, Kołodziej P, Kocki J, Bogucka-Kocka A (2019) Cytotoxic and Proapoptotic Activity of Sanguinarine, Berberine, and Extracts of Chelidonium majus L. and Berberis thunbergii DC. toward Hematopoietic Cancer Cell Lines. Toxins (Basel) 11 (9). doi: 10.3390/toxins11090485
25. Almatroodi SA, Alsahli MA, Rahmani AH (2022) Berberine: An Important Emphasis on Its Anticancer Effects through Modulation of Various Cell Signaling Pathways. Molecules 27 (18). doi: 10.3390/molecules27185889
26. Mohammadlou M, Abdollahi M, Hemati M, Baharlou R, Doulabi EM, Pashaei M, Ghahremanfard F, Faranoush M, Kokhaei P (2021) Apoptotic effect of berberine via Bcl-2, ROR1, and mir-21 in patients with B-chronic lymphocytic leukemia. Phytother Res 35 (4): 2025-2033. doi: 10.1002/ptr.6945
27. Ouyang S, Li H, Lou L, Huang Q, Zhang Z, Mo J, Li M, Lu J, Zhu K, Chu Y, Ding W, Zhu J, Lin Z, Zhong L, Wang J, Yue P, Turkson J, Liu P, Wang Y, Zhang X (2022) Inhibition of STAT3-ferroptosis negative regulatory axis suppresses tumor growth and alleviates chemoresistance in gastric cancer. Redox Biol 52: 102317. doi: 10.1016/j.redox.2022.102317
28. Adhami VM, Aziz MH, Mukhtar H, Ahmad N (2003) Activation of prodeath Bcl-2 family proteins and mitochondrial apoptosis pathway by sanguinarine in immortalized human HaCaT keratinocytes. Clinical Cancer Research 9 (8): 3176-3182. doi:
29. Liu L, Sun L, Zheng J, Cui L (2021) Berberine modulates Keratin 17 to inhibit cervical cancer cell viability and metastasis. J Recept Signal Transduct Res 41 (6): 521-531. doi: 10.1080/10799893.2020.1830110
30. Zhang C, Sheng J, Li G, Zhao L, Wang Y, Yang W, Yao X, Sun L, Zhang Z, Cui R (2019) Effects of Berberine and Its Derivatives on Cancer: A Systems Pharmacology Review. Front Pharmacol 10: 1461. doi: 10.3389/fphar.2019.01461